

# Observation of Mode-Specific Vibrational Autodetachment from Dipole-Bound States of Cold Anions\*\*

Hong-Tao Liu, Chuan-Gang Ning, Dao-Ling Huang, Phuong Diem Dau, and Lai-Sheng Wang\*

Molecules with sufficiently large dipole moments were predicted to form weakly bound negative ions in the dipolar field<sup>[1–4]</sup> and such dipole-bound anions have been observed and characterized experimentally.<sup>[5–10]</sup> Negative ions with dipolar molecular cores can have excited dipole-bound states (DBSs) near the detachment threshold, analogous to Rydberg states in neutral molecules. DBSs in excited anions were first observed as resonances in photodetachment cross-sections.<sup>[11–13]</sup> Ultrahigh resolution spectroscopy has been reported on excited DBSs of a number of anions near their detachment threshold by autodetachment.<sup>[14–16]</sup> The theory for autoionization from Rydberg states was first developed by Berry,<sup>[17]</sup> who predicted a  $\Delta\nu = -1$  vibrational propensity rule, that is, the Rydberg state undergoes a vibrational relaxation by one vibrational quantum in the molecular core during autoionization, in which the vibrational energy is transferred to the Rydberg electron. The  $\Delta\nu = -1$  propensity rule has been observed in autoionization of numerous molecules<sup>[18–20]</sup> and mode-specific autoionization has been observed by photoelectron spectroscopy,<sup>[21]</sup> in which the kinetic energies of the outgoing electrons are measured. The same  $\Delta\nu = -1$  propensity rule should apply in autodetachment from DBSs of excited anions<sup>[22]</sup> and has been inferred in previous studies.<sup>[13,16]</sup> However, the electron kinetic energies of the outgoing autodetached electrons from the excited DBSs have not been measured by electron spectroscopy.

All prior studies of DBSs in excited anions are dominated by rotational effects<sup>[23,24]</sup> and pure vibrational autodetachment from DBSs has not been reported, even though vibrational autodetachment has been observed in weakly bound anions and has been used effectively as a spectroscopic tool for anions.<sup>[25–27]</sup> Here we report the direct observation of pure vibrational autodetachment from DBSs of cryogenically cooled phenoxide anions using high-resolution photoelectron imaging. Autodetachment from eight vibrational levels of the DBS in optically excited phenoxide anions are observed and the  $\Delta\nu = -1$  propensity rule is found to be strictly obeyed. Three vibrational modes, which have weak Franck–Condon factors in the nonresonant photodetachment, are observed to

be dramatically enhanced. Excitation to the bound ground vibrational level of the DBSs of phenoxide is observed using resonant two-photon detachment, allowing the binding energy of the DBSs to be directly measured.

The phenoxy radical ( $C_6H_5O^\bullet$ ) is an important transient specie involved in numerous environmental and biological processes. Its vibrational spectroscopy has been studied in solution and in argon matrices.<sup>[28,29]</sup> Photoelectron spectroscopy (PES) of the phenoxide anion ( $C_6H_5O^-$ ) consists of an extensive vibrational progression in the  $\nu_{11}$  mode.<sup>[30]</sup> A recent high-resolution PE imaging study of phenoxide yielded an accurate electron affinity ( $18178 \pm 7 \text{ cm}^{-1}$ ) and a  $\nu_{11}$  vibrational frequency ( $519 \text{ cm}^{-1}$ ) for the phenoxy radical.<sup>[31]</sup> The current experiments are carried out using a PES apparatus equipped with an electrospray ionization source,<sup>[32]</sup> a cryogenically controlled ion trap,<sup>[33]</sup> and a high-resolution PE imaging system.<sup>[34]</sup> The phenoxide anions were produced by electrospray of a mixed phenol/sodium hydroxide solution. Anions from the electrospray source were transported into a temperature-controlled ion trap, where they were accumulated and cooled for 0.1 s before being ejected into the extraction zone of a time-of-flight mass spectrometer. A dye laser was used in the current study and the imaging system was calibrated using the known spectra of  $Au^-$ . The resolution of the imaging system has been described recently<sup>[34]</sup> and can reach about  $2 \text{ cm}^{-1}$  for low-energy electrons.

The PE images and spectra at 20 K are shown in Figure 1 at four photon energies. These data are similar to those reported recently,<sup>[31]</sup> with two important differences. First, the cryogenically cooled ions completely eliminate the vibrational hot bands and result in narrower line widths. The  $0 \leftarrow 0$  transition ( $0_0^0$ ) in Figure 1a reveals rotational contours (see inset) and defines a more accurate electron affinity of  $18173 \pm 3 \text{ cm}^{-1}$  for the phenoxy radical. More importantly, in addition to the dominating  $\nu_{11}$  vibrational progression, vibrational transitions with weak Franck–Condon factors are observed, that is, modes  $\nu_9$ ,  $\nu_{10}$ , and  $\nu_{18}$  and their combination bands with mode  $\nu_{11}$ . The modes  $\nu_9$  and  $\nu_{10}$  are both totally symmetric with  $a_1$  symmetry,<sup>[29,35]</sup> similar to mode  $\nu_{11}$ , and are allowed transitions. However, mode  $\nu_{18}$  has  $b_1$  symmetry and its activity must be due to vibronic couplings, as observed recently in high-resolution PE imaging of other small polyatomic anions.<sup>[36]</sup> The angular distributions of all the vibrational peaks because of the  $a_1$  modes display s- plus d-orbital characters,<sup>[31]</sup> consistent with the p-type orbital from which the electron is detached. The angular distributions of the vibrational peaks because of the  $\nu_{18}$  mode are different, displaying distinct p-orbital character (Figure 1). The different angular distributions for the different vibrational modes are interesting and can be used in vibrational assignments in

[\*] Dr. H. T. Liu, D. L. Huang, P. D. Dau, Prof. Dr. L. S. Wang  
Department of Chemistry, Brown University  
Providence, RI 02912 (USA)  
E-mail: Lai-Sheng\_Wang@brown.edu

Prof. Dr. C. G. Ning  
Department of Physics  
State Key Laboratory of Low-Dimensional Quantum Physics  
Tsinghua University, Beijing, 100084 (China)

[\*\*] This work was supported by the National Science Foundation (grant number CHE-1049717).

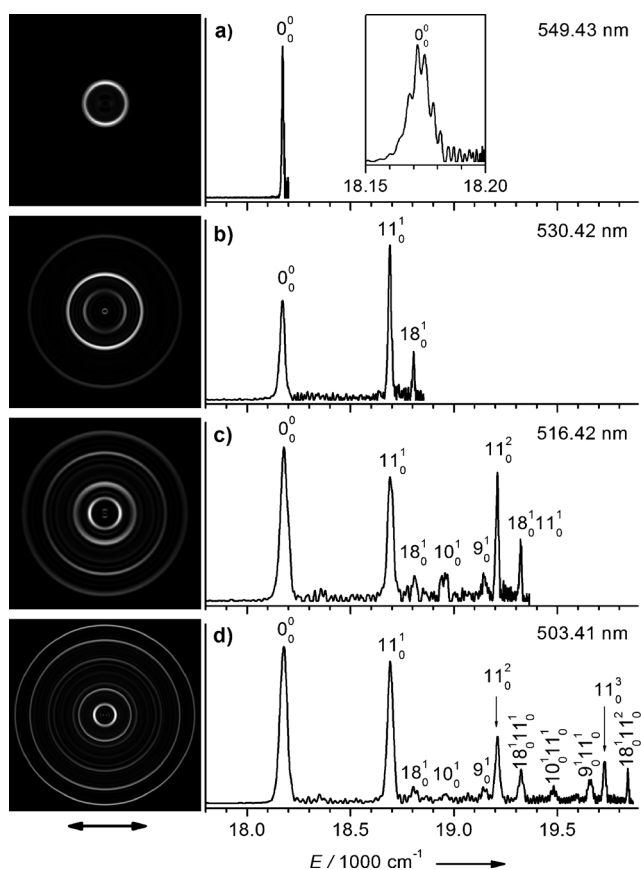


**Figure 1.** Photoelectron imaging of  $\text{C}_6\text{H}_5\text{O}^-$  at 20 K and a) 549.43, b) 530.42, c) 516.42, and d) 503.41 nm. The PE images after inverse-Abel transformation are shown on the left side. The laser polarization is given by the double arrow below the images. The PE spectra are obtained by integrating the signals from the respective images circumferentially. The electron kinetic energy is proportional to the square of the radius ( $r^2$ ) and is calibrated by the known spectra of  $\text{Au}^-$ . The binding energy spectra are obtained by subtracting the kinetic energy spectrum from the respective detachment photon energies. The observed vibrational structures are labeled according to the vibrational modes of the phenoxy radical. Note the significant threshold enhancement observed in (b–d). The angular distributions of all vibrational transitions are perpendicular except for those involving mode  $\nu_{18}$ , which display maximum intensity in the directions parallel to the laser polarization; see (b–d).

PE imaging of complex anions. The vibrational frequency of  $519\text{ cm}^{-1}$  obtained for the main  $\nu_{11}$  vibrational progression in the current study is in good agreement with the recent report.<sup>[31]</sup> The vibrational frequencies we obtained for modes  $\nu_9$ ,  $\nu_{10}$ , and  $\nu_{18}$  are  $972$ ,  $790$ , and  $632\text{ cm}^{-1}$ , respectively, but there have been no prior experimental measurements for these three modes in the gas phase. The frequencies for modes  $\nu_9$  and  $\nu_{18}$  are in good agreement with the prior infrared absorption measurements in argon matrices ( $\nu_9 = 977\text{ cm}^{-1}$  and  $\nu_{18} = 635\text{ cm}^{-1}$ ).<sup>[29]</sup> However, the frequency we measured for  $\nu_{10}$  is lower than the matrix value of  $813\text{ cm}^{-1}$ , but in good accord with the calculated  $\nu_{10}$  frequency.<sup>[31,35]</sup>

At certain wavelengths the PE images and spectra are dramatically different, as shown in Figure 2, where the  $0_0^0$  transition is plotted as the origin so that the vibrational spacing in wavenumbers for the higher binding energy peaks

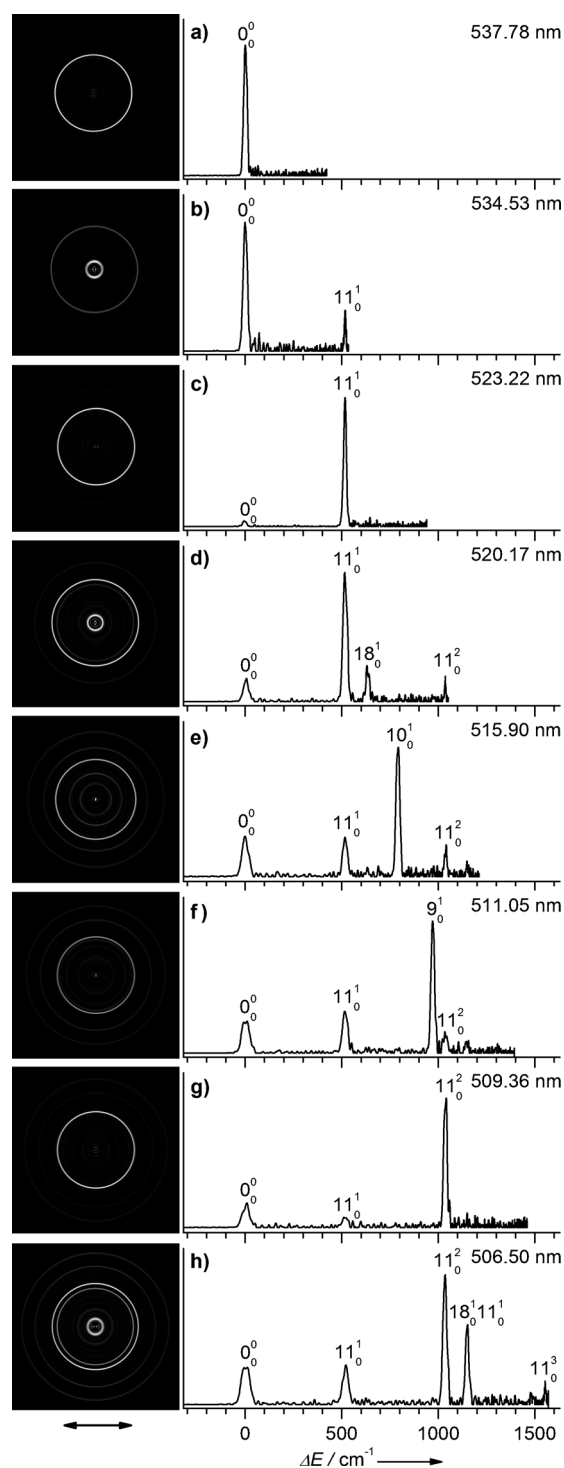


**Figure 2.** Resonant photoelectron imaging of  $\text{C}_6\text{H}_5\text{O}^-$  at 20 K and a) 537.78, b) 534.53, c) 523.22 nm, d) 520.17 nm, e) 515.90, f) 511.05, g) 509.36, and h) 506.50 nm. Each wavelength is in resonance with a vibrational level of the dipole-bound state (see Figure 4). The photoelectron signals come from both direct detachment (weak) and autodetachment through the dipole-bound state, which dominates the spectra. The photoelectron images after inverse-Abel transformation are shown on the left side. The binding energy spectra are plotted by referencing to the  $0_0^0$  transition. The angular distributions of the predominating autodetachment peaks are isotropic, while the direct detachment channels are perpendicular [see the  $11_0^1$  transition in (b)].

can be directly read off the axis. When we tuned the detachment laser to near 538 nm, we obtained a single peak corresponding to the  $0_0^0$  transition in the PE image (Figure 2a). The detachment cross-section at this wavelength is significantly higher and the angular distribution is isotropic, suggesting that the electron signal must be due to autodetachment from a resonantly excited state of the phenoxide anion. We scanned the wavelength around 538 nm by monitoring the electron signal of the  $0_0^0$  transition and obtained a sharp excitation spectrum ( $\approx 10 \text{ cm}^{-1}$  in width) to the autodetaching state, labeled as  $11'_0^1$  in Figure 3. The inset of Figure 3 reveals fine structures in this peak, which are similar to the  $0_0^0$  peak observed in the PE image (inset of Figure 1a) and are

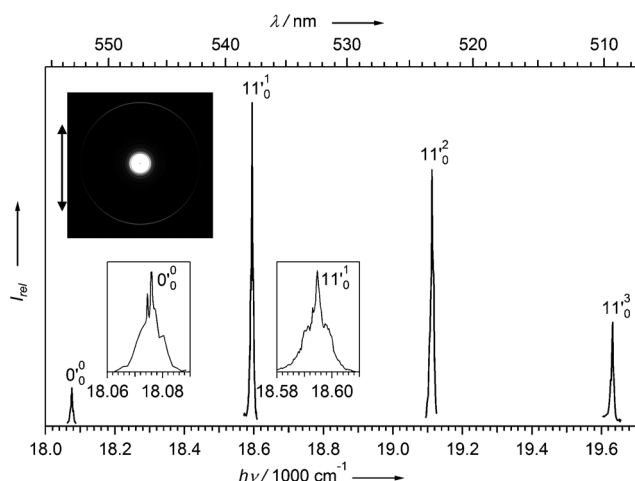


**Figure 3.** Excitation spectra to the  $\nu_{11}$  vibrational levels of the dipole-bound state of  $\text{C}_6\text{H}_5\text{O}^-$ . The transitions to the  $11'_0^1$ ,  $11'_0^2$ , and  $11'_0^3$  levels were obtained by monitoring the autodetachment signals, whereas the transition to the bound  $0_0^0$  level was obtained by monitoring the two-photon detachment transition (outer ring of the photoelectron image in the inset). The  $0_0^0$  and  $11'_0^1$  transitions are expanded in the inset, showing fine features possibly because of the rotational profile. The spectra were obtained for anions cooled to 4.4 K (ion trap temperature). The double arrow next to the photoelectron image indicates the laser polarization. Note that the two-photon detachment used to probe the  $0_0^0$  level was very weak.

likely due to the rotational profile. The center of this peak is at 537.78 nm and the PE image at this wavelength, shown in Figure 2a, should be due to both direct detachment from the ground state of the phenoxide anion and autodetachment from the excited state of phenoxide to the ground vibrational level of the phenoxy, giving rise to an electron kinetic energy of  $422 \text{ cm}^{-1}$ .

The phenoxy radical has a dipole moment of 4.0 Debye,<sup>[37]</sup> and is capable of supporting a DBS, even though it was not observed previously in the photodetachment cross-section measurement.<sup>[38]</sup> The resonance at 537.78 nm should correspond to a vibrational level of the DBS, most likely of the  $\nu_{11}$  mode, because it has the strongest Franck–Condon factors. Inasmuch as the structure of the DBS should be similar to the neutral phenoxy radical, the vibrational frequencies of the DBS should also be similar to that of the neutral radical. Hence, we tuned our laser to 523.22 nm, which is  $519 \text{ cm}^{-1}$  or

one vibrational quantum above the 537.78 nm resonance, and obtained the PE image presented in Figure 2c, which shows a strong  $11_0^1$  transition, suggesting an autodetachment from the vibrationally excited level of the DBS of phenoxide with a  $\Delta\nu = -1$  propensity. We scanned the wavelength around 523 nm by monitoring the electron signals corresponding to the  $11_0^1$  peak and obtained the excitation spectrum of the autodetaching vibrational level, shown as  $11'_0^2$  in Figure 3. We further tuned our laser to 509.36 nm,  $519 \text{ cm}^{-1}$  above the 523.22 nm resonance and obtained the PE image displayed in Figure 2g, which shows that the  $11_0^2$  peak is significantly enhanced, suggesting again an autodetachment from a vibrationally excited DBS with a  $\Delta\nu = -1$  propensity. The corresponding excitation spectrum by scanning the laser around 509 nm while monitoring the electron signals of the  $11_0^2$  vibrational peak is shown in Figure 3 as  $11'_0^3$ .

Figure 4 shows the energy level diagram of the direct detachment from the ground state of the phenoxide anion to the vibrational levels of the neutral phenoxy radical and the autodetachment resonant levels described above (the thick vertical arrows). The autodetachment from the DBS vibrational levels of the  $\nu_{11}$  mode to the corresponding phenoxy radical vibrational levels obeys the  $\Delta\nu = -1$  propensity rule, each autodetaching to the nearest vibrational level of the neutral phenoxy radical and producing an electron kinetic energy of  $422 \text{ cm}^{-1}$ . Thus, the 537.78 nm resonance is  $422 \text{ cm}^{-1}$  above the ground vibrational level of the phenoxy radical. If the phenoxide anion has a true dipole-bound excited state, then the 537.78 nm resonance must correspond to a vibrationally excited state of the DBS. If the 537.78 nm resonance is the  $\nu' = 1$  level of the  $\nu_{11}'$  mode ( $11'_0^1$ ) of the DBS, then the ground

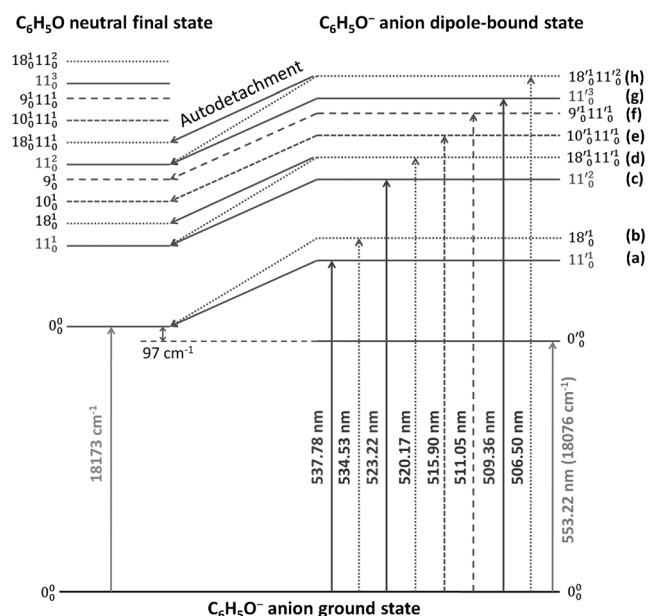


**Figure 4.** Energy level diagrams for the direct detachment to the vibrational levels of the phenoxy radical (left) and the vibrational levels of the dipole-bound state. The vertical arrows represent the resonant excitations. Autodetachment transitions from the dipole-bound state to the vibrational levels of the phenoxy radical are indicated. The letters in parentheses next to the vibrational levels of the dipole-bound state correspond to the spectra in Figure 2.

vibrational level of the DBS should be  $519\text{ cm}^{-1}$  below at  $553.22\text{ nm}$ , giving rise to a binding energy of  $97\text{ cm}^{-1}$  ( $519\text{ cm}^{-1}$ – $422\text{ cm}^{-1}$ ) for the DBS. Indeed, when we tuned our laser to  $553.22\text{ nm}$ , we observed a weak two-photon detachment signal (see the image in the inset of Figure 3). Scanning the laser around  $553.22\text{ nm}$  by monitoring the two-photon detachment signal, we obtained the spectrum shown in Figure 3 labeled as  $0_0^0$ . The inset in Figure 3 shows the rotational profile of the two-photon detachment spectrum, which is similar to the autodetachment spectrum of the  $11'_0^1$  level. To confirm that the  $553.22\text{ nm}$  excitation corresponds to the ground vibrational level of the DBS, we tuned our laser to  $566.03\text{ nm}$  or  $519\text{ cm}^{-1}$  below  $553.22\text{ nm}$  and did not observe any two-photon detachment signals. Thus, the DBS of phenoxide is  $18076\text{ cm}^{-1}$  ( $553.22\text{ nm}$ ) above the ground state of the anion with a binding energy of  $97\text{ cm}^{-1}$ . Note that the angular distributions of all the autodetachment transitions are isotropic (Figure 2a, c, and g), whereas the two-photon signals display a parallel transition (Figure 3).

In addition to the resonances corresponding to the  $\nu_{11}$  mode, we observed resonant excitations to  $18'_0^1$  (Figure 2b) and combination bands of mode  $\nu_{11}$  with modes  $\nu_{18}$ ,  $\nu_{10}$ , and  $\nu_9$ :  $18'_0^1 11'_0^1$  (Figure 2d),  $10'_0^1 11'_0^1$  (Figure 2e),  $9'_0^1 11'_0^1$  (Figure 2f), and  $18'_0^1 11'_0^2$  (Figure 2h). In each case, the  $\Delta\nu = -1$  vibrational propensity rule is obeyed, as shown in Figure 4. The  $\nu_9$ ,  $\nu_{10}$ , and  $\nu_{18}$  modes have very weak Franck–Condon factors, but they are enhanced by the autodetachment because of resonance absorption through DBSs, allowing their frequencies to be accurately measured. In the cases of resonant excitations to the  $10'_0^1 11'_0^1$  (Figure 2e) and  $9'_0^1 11'_0^1$  (Figure 2f) combination levels, autodetachment from mode  $\nu_{11}$  is strongly favored.

The current experiment reveals mode-specific autodetachment from a dipole-bound anion for an extensive set of vibrational levels. The vibrational frequencies of the DBS are found to be similar to those of the neutral radical, suggesting that the dipole-bound electron has little effect to the neutral core and providing direct evidence for the analogy of DBS and the Rydberg state in neutral molecules. There are many dipolar molecular radicals, which should support excited dipole-bound states. The DBS can be used to probe the vibrational structures of the radicals by resonant-enhanced autodetachment. Pump–probe experiments will be possible to investigate the dynamics of the excited dipole-bound states, providing a diverse set of systems to study vibronic couplings.

Received: May 31, 2013  
 Published online: July 14, 2013

**Keywords:** dipole-bound states · electron autodetachment · phenoxides · photoelectron spectroscopy · radicals

[1] A. S. Wightman, *Phys. Rev.* **1950**, *77*, 521.

- [2] R. F. Wallis, R. Herman, H. W. Milnes, *J. Mol. Spectrosc.* **1960**, *4*, 51.  
 [3] O. H. Crawford, *Mol. Phys.* **1971**, *20*, 585.  
 [4] W. R. Garrett, *Chem. Phys. Lett.* **1970**, *5*, 393.  
 [5] J. A. Stockdale, F. J. Davis, R. N. Compton, C. E. Klots, *J. Chem. Phys.* **1974**, *60*, 4279.  
 [6] H. Haberland, C. Ludewigt, H. G. Schindler, D. R. Worsnop, *J. Chem. Phys.* **1984**, *81*, 3742.  
 [7] C. Desfrancois, B. Baillon, J. P. Schermann, S. T. Arnold, J. H. Hendricks, K. H. Bowen, *Phys. Rev. Lett.* **1994**, *72*, 48.  
 [8] J. H. Hendricks, S. A. Lyapustina, H. L. de Clercq, J. T. Snodgrass, K. H. Bowen, *J. Chem. Phys.* **1996**, *104*, 7788.  
 [9] C. Desfrancois, H. Abdoul-Carime, J. P. Schermann, *Int. J. Mod. Phys. B* **1996**, *10*, 1339.  
 [10] N. I. Hammer, R. J. Hinde, R. N. Compton, K. Dirí, K. D. Jordan, D. Radisic, S. T. Stokes, K. H. Bowen, *J. Chem. Phys.* **2004**, *120*, 685.  
 [11] A. H. Zimmerman, J. I. Brauman, *J. Chem. Phys.* **1977**, *66*, 5823.  
 [12] R. L. Jackson, P. C. Hiberty, J. I. Brauman, *J. Chem. Phys.* **1981**, *74*, 3705.  
 [13] D. M. Wetzel, J. I. Brauman, *J. Chem. Phys.* **1989**, *90*, 68.  
 [14] K. R. Lykke, R. D. Mead, W. C. Lineberger, *Phys. Rev. Lett.* **1984**, *52*, 2221.  
 [15] K. R. Lykke, D. M. Neumark, T. Andersen, V. J. Trapa, W. C. Lineberger, *J. Chem. Phys.* **1987**, *87*, 6842.  
 [16] K. Yokoyama, G. W. Leach, J. B. Kim, W. C. Lineberger, A. I. Boldyrev, M. Gutowski, *J. Chem. Phys.* **1996**, *105*, 10706.  
 [17] R. S. Berry, *J. Chem. Phys.* **1966**, *45*, 1228.  
 [18] J. Berkowitz, W. A. Chupka, *J. Chem. Phys.* **1969**, *51*, 2341.  
 [19] P. M. Dehmer, W. A. Chupka, *J. Chem. Phys.* **1977**, *66*, 1972.  
 [20] H. Matsui, E. R. Grant, *J. Chem. Phys.* **1996**, *104*, 42.  
 [21] S. T. Pratt, *Annu. Rev. Phys. Chem.* **2005**, *56*, 281.  
 [22] J. Simons, *J. Am. Chem. Soc.* **1981**, *103*, 3971.  
 [23] D. C. Clary, *J. Phys. Chem.* **1988**, *92*, 3173.  
 [24] J. Simons, *J. Chem. Phys.* **1989**, *91*, 6858.  
 [25] D. M. Neumark, K. R. Lykke, T. Andersen, W. C. Lineberger, *J. Chem. Phys.* **1985**, *83*, 4364.  
 [26] J. M. Weber, W. H. Robertson, M. A. Johnson, *J. Chem. Phys.* **2001**, *115*, 10718.  
 [27] C. L. Adams, H. Schneider, J. M. Weber, *J. Phys. Chem. A* **2010**, *114*, 4017.  
 [28] A. Mukherjee, M. L. McGlashen, T. G. Spiro, *J. Phys. Chem.* **1995**, *99*, 4912.  
 [29] J. Spanget-Larsen, M. Gil, A. Gorski, D. M. Blake, J. Waluk, J. G. Radziszewski, *J. Am. Chem. Soc.* **2001**, *123*, 11253.  
 [30] R. F. Gunion, M. K. Gilles, M. L. Polak, W. C. Lineberger, *Int. J. Mass Spectrom. Ion Processes* **1992**, *117*, 601.  
 [31] J. B. Kim, T. I. Yacovitch, C. Hock, D. M. Neumark, *Phys. Chem. Chem. Phys.* **2011**, *13*, 17378.  
 [32] L. S. Wang, C. F. Ding, X. B. Wang, S. E. Barlow, *Rev. Sci. Instrum.* **1999**, *70*, 1957.  
 [33] X. B. Wang, L. S. Wang, *Rev. Sci. Instrum.* **2008**, *79*, 073108.  
 [34] I. León, Z. Yang, L. S. Wang, *J. Chem. Phys.* **2013**, *138*, 184304.  
 [35] D. M. Chipman, R. Liu, X. Zhou, P. Pulay, *J. Chem. Phys.* **1994**, *100*, 5023.  
 [36] E. Garand, T. I. Yacovitch, D. M. Neumark, *J. Chem. Phys.* **2008**, *129*, 074312.  
 [37] The dipole moment of the phenoxy radical is not known. This value is calculated using density functional theory with the B3LYP hybrid functional.  
 [38] J. H. Richardson, L. M. Stephenson, J. I. Brauman, *J. Am. Chem. Soc.* **1975**, *97*, 2967.